Journal of Thermal Analysis, Vol. 53 (1998) 397-410

Dedicated to Professor Ferenc Paulik on the occasion of his 75th birthday

THERMAL DECOMPOSITION OF $BaC_2O_4 \cdot 0.5H_2O$ STUDIED BY STEPWISE ISOTHERMAL ANALYSIS AND NON-ISOTHERMAL THERMOGRAVIMETRY

F. Chen[1*], *O. T. Sørensen*[2], *G. Meng*[1] *and D. Peng*[1]

[1]Department of Materials Science and Engineering, University of Science and Technology of China, Hefei, Anhui, 230026, P. R. China
[2]Materials Department, Risø National Laboratory, DK–4000 Roskilde, Denmark

Abstract

Thermal decomposition of $BaC_2O_4 \cdot 0.5H_2O$ in air was studied by a combination of stepwise isothermal analysis (SIA) and non-isothermal thermogravimetry. The results from both techniques show that the crystal water is released in one step and that anhydrous barium oxalate is decomposed in one step, while $BaCO_3$ decomposes in three steps to BaO, forming two intermediate compounds with the formulas of $BaCO_3 \cdot (BaO)_2$ and $(BaCO_3)_{0.5} \cdot (BaO)_{2.5}$. Reaction mechanism analyses using the data from SIA measurements show that the controlling mechanism for all the five decomposition steps in isothermal conditions is a two dimensional phase-boundary controlled process. Kinetic parameters are obtained for the five decomposition steps from the non-isothermal thermogravimetric data.

Keywords: barium oxalate, kinetics, non-isothermal thermogravimetry, stepwise isothermal analysis, thermal decomposition

Introduction

Thermal decomposition studies of oxalates are of importance in synthesizing double or multicomponent oxides [1–2]. High purity barium titanates, barium cerates and barium zirconates of perfect stoichiometry can be prepared from mixed metal oxalate systems [3–6] Accordingly, it is of great interest to investigate the thermal decomposition behaviour of barium oxalate hemihydrate.

The stepwise isothermal analysis (SIA) technique, which was introduced by Sørensen in the late seventies [7–8], has been proved to be an effective method in determining the reaction mechanism. In contrast to conventional thermal analy-

* Present address: School of Materials Science and Engineering, Georgia Institute of Technology, Atlanta GA30332

1418–2874/98/ $ 5.00

Akadémiai Kiadó, Budapest
Kluwer Academic Publishers, Dordrecht

sis in which the sample is heated at a constant rate, the overall heating in SIA is controlled by the rate of the reactions taking place in the sample. This technique, which can also be termed as 'sample controlled thermal analysis', has the advantage that close-lying reactions can be resolved and the overlaps generally observed by standard thermal analysis measurements can be avoided [9]. However, the main draw back of the SIA technique is that kinetic parameters such as the activation energies and the pre-exponential factors can not be generally obtained if the reaction takes place in one isothermal step [10].

Non-isothermal thermogravimetry (with linear temperature increase) is widely used as a tool for deriving kinetic parameters such as the activation energy and pre-exponential factor for solid state decompositions. The advantages of determining kinetic parameters by non-isothermal technique rather than by isothermal study are the following:

(1) the kinetics can be established over an entire temperature range in a continuous manner;

(2) non-isothermal thermogravimetry demands less time-consuming experiments than does the isothermal technique;

(3) it is possible to obtain a lot of information with a single sample, i.e., thermal parameters such as the temperature at maximum decomposition rate, characteristic temperatures, and kinetic parameters and

(4) it is possible to remove the problem of selecting several identical samples as in isothermal analysis [11, 12].

But the disadvantages of this technique are that overlapping between close lying reactions can not be avoided.

From the above considerations, it is clear that SIA and non-isothermal thermogravimetry techniques supplement each other in resolving the reaction mechanisms and in determining the kinetic parameters.

In the present work, the thermal decomposition process of barium oxalate hemihydrate was investigated by employing both SIA and non-isothermal thermogravimetry techniques in order to elucidate the reaction mechanism and to obtain the kinetic parameters.

Kinetic analysis

For the solid thermal decomposition considered in the present work, as expressed by the stoichiometric equation:

$$A_{(s)} = B_{(s)} + C_{(g)} \tag{1}$$

the kinetic equation for isothermal conditions can be expressed in the integral form as:

$$\kappa t = g(\alpha) \tag{2}$$

or the differential form as:

$$\frac{d\alpha}{dt} = \kappa f(\alpha) \tag{3}$$

where $g(\alpha)$ and $f(\alpha)$ are the integral and differential forms of α, the fraction decomposed in time t and κ is the rate constant as expressed by the Arrhenius equation:

$$\kappa = A\exp\left(-\frac{E}{RT}\right) \tag{4}$$

where A is the pre-exponential factor (frequency factor) and E is the activation energy.

The forms of $g(\alpha)$ and $f(\alpha)$ depend on the type of the rate-limiting process, i.e., the slowest process, that controls the overall reaction. It is possible to evaluate the type of the controlling mechanism from the $g(\alpha)$ *vs.* t and $f(\alpha)$ *vs.* $d\alpha/dt$ plots which according to Eqs (2) and (3), should be linear for the correct mechanisms.

It has been pointed out that the above relationships (Eqs (2) and (3)) in isothermal conditions can also be established for non-isothermal cases [13]. Since thermogravimetric analysis in non-isothermal conditions is carried out at a constant heating rate, $q=dT/dt$, the substitution $dt=dT/q$ can be made, and the following differential equation is obtained

$$\frac{d\alpha}{dT}\frac{1}{f(\alpha)} = \frac{A}{q}\exp\left(-\frac{E}{RT}\right) \tag{5}$$

or

$$\frac{d\alpha}{f(\alpha)} = \frac{A}{q}\exp\left(-\frac{E}{RT}\right)dT \tag{6}$$

Taking logarithm, Eq. (5) becomes

$$\ln\left(\frac{d\alpha}{dT}\frac{1}{f(\alpha)}\right) = \ln\left(\frac{A}{q}\right) - \frac{E}{RT} \tag{7}$$

This is termed as the differential method since it employs the differential form of $f(\alpha)$. By plotting $\ln[(d\alpha/dT)\ 1/f(\alpha)]$ *vs.* $1/T$, one can obtain a linear curve when the correct mechanism is chosen. The activation energy E and the pre-exponential factor A can then be calculated from the slope and the intercept of the linear curve, respectively.

When integrated between proper limits, Eq. (6) gives

$$\int_0^{\alpha} \frac{d\alpha}{f(\alpha)} = g(\alpha) = \frac{A}{q}\int_0^{T} \exp\left(-\frac{E}{RT}\right) dT \tag{8}$$

Based on Eq. (8), Coats and Redfern [14] derived the following equation, which is termed as the integral method

$$\ln\left[\frac{g(\alpha)}{T^2}\right] = \ln\frac{AR}{qE}\left[1 - \frac{2RT}{E}\right] - \frac{E}{RT} \tag{9}$$

When plotting $\ln[g(\alpha)/T^2]$ *vs.* $1/T$, a linear curve will be obtained for the correct mechanisms. The slope of the curve equals to $-E/R$. The intercept equals to $\ln[(AR/qE)(1-2RT/E)]$, thus allowing calculation of the activation energy E and pre-exponential factor A. In this study the average temperature for the reaction range was used for the calculation of the pre-exponential factor A.

Experimental

Barium oxalate hemihydrate powders were prepared by oxalate precipitation using the homogeneous solution method [4]. The powder has an average particle size of 0.3 μm as determined by scanning electron microscopy (SEM; JEOL JSM-840). TG–DTA measurements were carried out on a fully computer-controlled simultaneous TG–DTA system (TG/DTA320U, Seiko Instruments, Japan). Powders (~23 mg) were loaded into open cylindrical alumina crucible at room temperature and then heated in air (200 ml min^{-1}) up to 1300°C, using either the SIA technique or the non-isothermal thermogravimetry technique. In the latter case, a constant heating rate of 2, 5 and 10°C min^{-1} was applied. Data of the mass change, temperature, time, DTA signal and mass change rate were recorded every second.

For the SIA technique, the sample was heated at a constant heating rate (2°C min^{-1} in this work) until the rate of mass change exceeded a preset limit (15 μg min^{-1} was adopted in this work). When this happened, heating was stopped and the reaction took place at a constant temperature until the rate of the mass change became smaller than a second preset limit, after which heating was resumed. In this work, the second limit was chosen as one-forth of the first limit in order to ensure completion of the reaction.

A computer program was developed for all the data manipulations. From the data obtained by the SIA technique, $g(\alpha)$ *vs.* t and $f(\alpha)$ *vs.* $d\alpha/dt$ were plotted from the measured mass changes for the most commonly used kinetic equations listed in Table 1. This allows a very detailed kinetic analysis involving many important mechanisms such as nucleation, phase boundary reaction or diffusion controlled

Table 1 Kinetic functions (differential and integral forms) used for the present analysis

Function No.	Name of function	Rate determining mechanism	$f(\alpha)$	$g(\alpha)$
1	Parabolic law	1-dimensional diffusion, D1	$1/\alpha$	$\alpha^2/2$
2	Valensi (Barrer) eqn.	2-dimensional diffusion, D2	$[-\ln(1-\alpha)]^{-1}$	$(1-\alpha)\ln(1-\alpha)+\alpha$
3	Jander eqn.	3-dimensional diffusion, D3	$(1-\alpha)^{2/3}[1-(1-\alpha)^{1/3}]^{-1}$	$3/2[1-(1-\alpha)^{1/3}]^2$
4	Ginstling-Brounshtein eqn.	3-dimensional diffusion, D4	$[(1-\alpha)^{-1/3}-1]^{-1}$	$3/2[(1-2/3\alpha)-(1-\alpha)^{2/3}]$
5	Avrami-Erofeev eqn.	nucleation followed by the growth of nuclei, A1 (one nucleus on each particle)	$(1-\alpha)$	$-\ln(1-\alpha)$
6	Avrami-Erofeev eqn.	nucleation followed by the growth of nuclei, A2 (two-dimensional growth of nuclei)	$(1-\alpha)[-\ln(1-\alpha)]^{1/2}$	$2[-\ln(1-\alpha)]^{1/2}$
7	Avrami-Erofeev eqn.	nucleation followed by the growth of nuclei, A3 (three-dimensional growth of nuclei)	$(1-\alpha)[-\ln(1-\alpha)]^{2/3}$	$3[-\ln(1-\alpha)]^{1/3}$
8		phase-boundary movement (cylindric symmetry)	$(1-\alpha)^{1/2}$	$2[1-(1-\alpha)^{1/2}]$
9		phase-boundary movement (spherical symmetry)	$(1-\alpha)^{2/3}$	$3[1-(1-\alpha)^{1/3}]$
10	Mampel power law	nucleation	1	α
11	Mampel power law	nucleation	$\alpha^{1/2}$	$2\alpha^{1/2}$
12	Mampel power law	nucleation	$\alpha^{2/3}$	$3\alpha^{1/3}$
13	Mampel power law	nucleation	$\alpha^{3/4}$	$4\alpha^{1/4}$

process. In non-isothermal thermogravimetry technique, both differential and integral methods are applied to derive kinetic parameters of E and $\ln A$ by using the $g(\alpha)$ and $f(\alpha)$ forms listed in Table 1.

Results and discussion

Decomposition process

Figure 1 shows the TG–DTG signals obtained in the non-isothermal thermogravimetry technique with the heating rate of 2°C min^{-1}. The TG–DTG curves using other heating rate have similar shapes, indicating that the thermal decomposition process of barium oxalate hemihydrate to barium oxide in the experimental temperature range may be described by the following five steps:

$$BaC_2O_4{\cdot}0.5H_2O \xrightarrow{1} BaC_2O_4 \xrightarrow{2} BaCO_3 \xrightarrow{3,4,5} BaO$$

Step 1 is due to the removal of crystal water. Step 2 is the result of the decomposition process of anhydrous barium oxalate to yield barium carbonate. Steps 3–5 correspond to the decomposition process of barium carbonate.

Figure 2 shows TG–DTA signals as a function of temperature obtained using the SIA technique. Five distinct isothermal mass loss steps appeared in barium oxalate hemihydrate thermal decomposition process. This is in consistence with the above results obtained by using the non-isothermal thermogravimetry technique, but the only difference is that the SIA technique can far better resolve the close-lying $BaCO_3$ decomposition steps and avoid the overlaps as observed in Fig. 1.

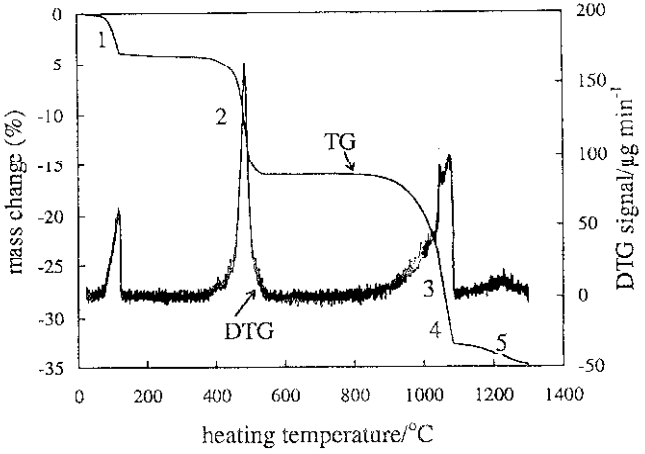

Fig. 1 TG–DTG diagrams of $BaC_2O_4{\cdot}0.5H_2O$ in air studied by non-isothermal thermogravimetry with a heating rate of 2°C min^{-1}

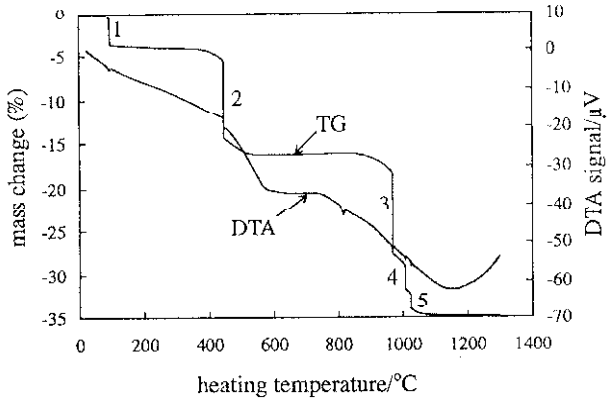

Fig. 2 TG–DTA diagrams of $BaC_2O_4 \cdot 0.5H_2O$ in air studied by stepwise isothermal analysis

Based on the results in Figs 1 and 2, the decomposition process of barium oxalate hemihydrate can be proposed to take place in the following five steps:

$$BaC_2O_4 \cdot 0.5H_2O \rightarrow BaC_2O_4 + 0.5H_2O \quad (1)$$

which corresponds to the first mass change step.

$$BaC_2O_4 \rightarrow BaCO_3 + CO \quad (2)$$

which corresponds to the second mass change step.

$$3BaCO_3 \rightarrow BaCO_3 \cdot (BaO)_2 + 2CO_2 \quad (3)$$

$$BaCO_3(BaO)_2 \rightarrow (BaCO_3)_{0.5} \cdot (BaO)_{2.5} + 1/2CO_2 \quad (4)$$

$$(BaCO_3)_{0.5} \cdot (BaO)_{2.5} \rightarrow 3BaO + 1/2CO_2 \quad (5)$$

The last three mass change steps correspond to the decomposition of $BaCO_3$ to BaO, revealing that intermediate compounds equivalent to the formula of $BaCO_3 \cdot (BaO)_2$ and $(BaCO_3)_{0.5}(BaO)_{2.5}$ were formed during the decomposition process. The SIA technique can effectively differentiate the overlapping reactions of $BaCO_3$ decomposition compared with that of non-isothermal thermogravimetry technique. The DTA signals in Fig. 2 show that all of the five decomposition steps as expressed in reactions (1)–(5) are endothermic reactions. The endothermic peak at 814°C in the DTA curve is the result of the phase transition of $BaCO_3$ from the orthorhombic to the rhombohedral and this agrees with that observed in conventional combined DTA–TG studies [15].

The thermal decomposition of $BaCO_3$ in the equilibrium $BaCO_3 \leftrightarrow BaO + CO_2$ has been investigated by Kelley and Anderson [16, 17] with the aim of determining some of the thermodynamic properties of BaO and $BaCO_3$. Following

Finkelstein [18], they assumed the existence of a basic carbonate, $BaCO_3 \cdot BaO$, in the solid phase since they observed a eutectic in the $BaCO_3$–BaO system. Later on, Hackspill and Wolf [19] and Baker [20] assigned the composition $2BaCO_3 \cdot BaO$ to the eutectic. In this work, from Figs 1 and 2, it can be undoubtedly seen that the thermal decomposition of $BaCO_3$ consists of three steps as expressed by reactions (3)–(5), indicating that intermediate compounds with the formula of $BaCO_3 \cdot (BaO)_2$ and $(BaCO_3)_{0.5} \cdot (BaO)_{2.5}$ exist during the thermal decomposition process. No signs of the intermediate compound with the composition either $BaCO_3 \cdot BaO$ or $2BaCO_3 \cdot BaO$ has been revealed in the present work. SIA technique demonstrates its advantages in separating these consecutive and close-lying reactions compared with the non-isothermal thermogravimetry technique.

Reaction mechanism–SIA technique

The data from the SIA measurements were fitted to Eqs (2) and (3) by the linear least-squares method using the different forms of $g(\alpha)$ and $f(\alpha)$ listed in Table 1. The controlling mechanism for reactions (1)–(5) was determined by the best fitting straight line with the highest correlation coefficient (r) from the $g(\alpha)$ *vs.* t and $f(\alpha)$ *vs.* $d\alpha/dt$ plots. It is generally possible to visually choose the best straight line, but the correlation coefficient, r, gives a quantitative value of judgement. Table 2 summarizes the r values obtained for the different reaction mechanisms for reactions (1)–(5) both from the integral and differential forms. It is obvious that for the proper functional forms of $g(\alpha)$ and $f(\alpha)$, the results obtained by integral method (Eq. (2)) should closely agree with those obtained by differential method (Eq (3)). This condition is satisfied when function no. 8 ($f(\alpha) = (1-\alpha)^{1/2}$, $g(\alpha) = 2[1-(1-\alpha)^{1/2}]$) is used for all the five isothermal steps. So, it may be concluded that the thermal decomposition process of barium oxalate hemihydrate, which takes place in five isothermal steps as described above, more probably is a phase-boundary controlled process which happens in two dimensions (cylindrical symmetry).

Kinetic parameters–non-isothermal thermogravimetry

Kinetic parameters, such as E and $\ln A$, are determined from the non-isothermal thermogravimetric data by using differential and integral methods, respectively. The original data for reactions (1)–(5) from raising-temperature thermogravimetry technique were analyzed by means of Eq. (7) and (9) with the possible forms of $f(\alpha)$ and $g(\alpha)$ listed in Table 1. The kinetic analyses were completed with the linear least-squares method.

As an example, analysis of the kinetic data is carried out on Reaction (1), i.e., the dehydration process of barium oxalate hemihydrate. The original data for this step from the non-isothermal thermogravimetric measurement are partially listed in Table 3. Using the possible forms of $f(\alpha)$ and $g(\alpha)$ from Table 1, the data

Table 2 The values of the correlation coefficient, r, for different integral ($g(\alpha)$ *vs.* t) and differentia. ($f(\alpha)$ *vs.* $d\alpha/dt$) plots for the five isothermal decomposition reactions of barium oxalate hemihydrate

Furction	Reaction (1)		Reaction (2)		Reaction (3)		Reaction (4)		Reaction (5)	
No.	integral	differential	integral	differential	integral	differential	integral	differential	integral	differential
1	0.9374	0.9433	0.9728	0.9638	0.9649	0.9569	0.9701	0.9815	0.9687	0.9541
2	0.9332	0.9359	0.9301	0.9315	0.9218	0.9451	0.9193	0.9775	0.9108	0.9545
3	0.9033	0.8953	0.901	0.9215	0.8975	0.9857	0.8866	0.9654	0.8671	0.9563
4	0.8659	0.8214	0.9328	0.8756	0.8857	0.9014	0.8736	0.8865	0.8423	0.9386
5	0.9840	0.9785	0.9787	0.9713	0.9741	0.9767	0.9648	0.9638	0.9454	0.9634
6	0.9844	0.9821	0.9748	0.9814	0.9881	0.9915	0.9761	0.9904	0.9731	0.9922
7	0.9839	0.9901	0.9872	0.9899	0.9873	0.9899	0.9904	0.9915	0.9929	0.9915
8	0.9904	0.9971	0.996	0.9937	0.9977	0.9929	0.9979	0.992.	0.9972	0.9938
9	0.9834	0.9924	0.9822	0.9893	0.9924	0.9934	0.9728	0.984.	0.9551	0.9617
10	0.9839	0.9763	0.9841	0.9754	0.9865	0.9817	0.9809	0.9876	0.9847	0.9756
11	0.9398	0.9457	0.9566	0.9786	0.757	0.9823	0.9641	0.9756	0.9463	0.9546
12	0.9540	0.9297	0.9576	0.9564	0.9798	0.9715	0.9678	0.9473	0.9546	0.8975
13	0.9348	0.9214	0.9457	0.9456	0.9868	0.9816	0.9679	0.9588	0.9645	0.9012

Table 3 Data for the thermal dehydration process of $BaC_2O_4 \cdot 0.5H_2O$ from the non-isothermal thermogravimetry

Data point	time/ s	T/ K	α	$(d\alpha/dT) \cdot 10^2$/ K^{-1}
1	140	348.18	0.0117	0.3225
2	280	352.29	0.0305	0.4770
3	420	356.50	0.0602	0.8038
4	560	360.62	0.1032	1.0916
5	700	364.82	0.1581	1.4984
6	840	369.02	0.2273	1.6456
7	980	373.23	0.3119	2.2327
8	1120	377.51	0.4128	2.7181
9	1260	381.92	0.5350	3.1477
10	1400	386.22	0.6759	3.6980
11	1540	390.46	0.8325	3.5382
12	1680	394.93	0.9831	2.6608

in Table 3 were analyzed by means of Eqs (7) and (9) and the results are shown in Table 4. It can be seen that the values of E and ln$A$ from the two methods are very close to each other, and that the linear correlation coefficients are better ($r \approx 1$) when the most probable mechanism is two-dimensional phase-boundary movement as expressed by function no. 8 ($f(\alpha)=(1-\alpha)^{1/2}$, $g(\alpha)=2[1-(1-\alpha)^{1/2}]$).

The other thermal decomposition processes described by Reactions (2)–(5) can be analyzed similarly. Table 5 summarizes the kinetic parameters and the most probable mechanisms for the different five thermal decomposition steps. The results in Table 5 show that the thermal decomposition of barium oxalate hemihydrate in non-isothermal conditions obeys the two-dimensional phase-boundary movement mechanism as expressed by function no. 8 ($f(\alpha)=(1-\alpha)^{1/2}$, $g(\alpha)=2[1-(1-\alpha)^{1/2}]$) for all the five thermal decomposition steps.

Kinetic analyses of the data from both isothermal and non-isothermal conditions thus suggest that all the five thermal decomposition steps of barium oxalate hemihydrate are controlled by two-dimensional phase-boundary movement. The rate controlling process might be the transfer of heat and/or mass to the reaction boundary, and/or by the transfer of gaseous products away from it. The activation energy for the dehydration process was determined to be 87.0±0.7 kJ mol^{-1}, which is close to that for the dehydration of calcium oxalate monohydrate, which is 88.44 kJ mol^{-1} [21]. The activation energy for the overall barium oxalate breakdown step is 296.0±14.6 kJ mol^{-1}, which is also close to that of the thermal decomposition of anhydrous calcium oxalate, 282.44 kJ mol^{-1} [22]. The activation energy for the decomposition of $BaCO_3$ to BaO obtained from the non-isothermal ther-

Table 4 Results of analyses of the thermal dehydration of $BaC_2O_4 \cdot 0.5H_2O$ by differential Eq. (7) and integral Eq. (9) methods

Mechanism	Function No.	Differential method			Integral method		
		E/ kJ mol^{-1}	ln$A$/ s^{-1}	r	E/ kJ mol^{-1}	ln$A$/ s^{-1}	r
Diffusion, D1	1	174.68	47.38	0.9605	179.22	42.21	0.9825
Diffusion, D2	2	195.41	54.4[illegible]	0.9779	192.66	46.79	0.9888
Diffusion, D3	3	221.25	62.05	0.9867	210.11	51.62	0.9939
Diffusion, D4	4	204.38	56.34	0.9825	168.18	41.47	0.9921
Nucleation and growth, A1	5	111.57	29.28	0.9695	111.58	20.85	0.9948
Nucleation and growth, A2	6	44.34	8.16	0.8183	52.70	3.76	0.9942
Nucleation and growth, A3	7	21.95	1.13	0.5477	33.07	–2.45	0.9934
Phase-boundary mouvement, R2	8	86.27	20.73	0.9907	97.66	17.49	0.9944
Phase-boundary mouvement, R3	9	94.71	23.58	0.9854	101.96	18.98	0.9935
Nucleation (power law)	10	60.97	12.18	0.9630	86.52	13.63	0.9812
Nucleation (power law)	11	–4.12	–5.43	0.8830	40.16	–0.7[illegible]	0.9780
Nucleation (power law)	12	–14.82	–11.30	0.7456	21.35	–8.62	0.9548
Nucleation (power law)	13	–23.47	–14.23	0.8430	14.21	–10.8[illegible]	0.9457

Table 5 Kinetic parameters for the decomposition of $BaC_2O_4 \cdot 0.5H_2O$ by analyses of data from the non-isothermal thermogravimetry

Decomp. step	Temp. range/ °C	Range of α	E/kJ mol^{-1}			ln$A$/s^{-1}			Mechanism
			differential	integral	average	differential	integral	average	
1	75–122	0.011–0.995	86.27	87.66	87.0±0.7	20.73	20.40	20.6±0.2	R2
2	391–535	0.051–0.936	310.58	281.38	296.0±14.6	42.85	37.97	40.3±2.5	R2
3	840–1040	0.024–0.926	283.84	312.53	298.2±14.3	19.08	23.60	21.3±2.3	R2
4	1041–1090	0.035–0.987	306.74	329.34	318.0±11.3	40.17	43.28	41.7±1.6	R2
5	1095–1250	0.051–0.876	341.90	322.32	332.1±9.8	20.08	22.41	21.2±1.2	R2

mogravimetry by Judd and Pope was 283 kJ mol^{-1} [23]. In this work, for the first time, we found that $BaCO_3$ decomposed in three steps, and the corresponding activation energies were 298.2±14.3, 318.0±11.3 and 332.1±9.8 kJ mol^{-1}, respectively. The activation energy increases consequently, indicating the relative difficulty in $BaCO_3$ decomposition process which takes place in three steps.

Conclusions

The SIA and non isothermal thermogravimetry results show that barium oxalate hemihydrate decomposes in five steps, in which the decomposition of barium carbonate proceeds in three consecutive steps, revealing the existence of two intermediate compounds of $BaCO_3 \cdot (BaO)_2$ and $(BaCO_3)_{0.5} \cdot (BaO)_{2.5}$. The SIA technique demonstrates its advantages in separating the consecutive and close-lying $BaCO_3$ decomposition reactions compared with the non-isothermal thermogravimetry.

Reaction mechanism analyses using the SIA data show that two-dimensional phase-boundary controlled process dominates in all the five decomposition steps. The rate controlling process might be the transfer of heat and/or mass to the reaction boundary, and/or by the transfer of gaseous products away from it. Kinetic parameters were obtained by analyses of the data from the non-isothermal thermogravimetry. The activation energies for the dehydration and the oxalate breakdown steps are 87.0±0.7 and 296.0±14.6 kJ mol^{-1}, respectively. The activation energies for the three $BaCO_3$ decomposition steps are 298.2±14.3, 318.0±11.3 and 332.1±9.8 kJ mol^{-1}, respectively. The activation energy increases consequently, indicating the relative difficulty in $BaCO_3$ decomposition process which takes place in three steps.

* * *

This work is supported by the Natural Science Foundation of China. Dr. N. Bonanos at Materials Department, Risø National Laboratory is acknowledged for his constant interest and encouragement to this work. Special thanks are given to P. Larsen, J. Kjøller, P. V. Jensen and T. R. Strauss for the experimental assistance.

Reference

1 S. Uma and J. Gopalakrishnan, J. Solid State Chem., 102 (1993) 332.
2 R. K. Sinha and S. K. Srivastava, Supercond. Sci. Technol., 6 (1993) 238.
3 M. Stockenhuber, H. Mayer and J. A. Lercher, J. Am. Ceram. Soc., 76 (1993) 1185.
4 F. L. Chen, P. Wang, O. T. Sørensen, G. Y. Meng and D. K. Peng, J. Mater. Chem., 7 (1997) 1533.
5 I. Aboltina, R. Ramata and I. Brante, Ferroelectrics, 141 (1993) 277.
6 V. B. Reddy and P. N. Kaushik, Thermochim. Acta, 83 (1985) 347.
7 O. T. Sørensen, J. Thermal Anal., 13 (1978) 429.
8 O. T. Sørensen, Thermochim. Acta, 29 (1979) 211.

9 O. T. Sørensen, J. Thermal Anal., 38 (1992) 213.
10 P. L. Husum and O. T. Sørensen, Thermochim. Acta, 114 (1987) 131.
11 D. W. Johnson and P. K. Gallapher, J. Phys. Chem., 76 (1972) 1474.
12 F. Carrasco, Thermochim. Acta, 213 (1993) 115.
13 T. P. Bagchi and P. K. Sen, Thermochim. Acta, 51 (1981) 175.
14 A. W. Coats and J. P. Redfern, Nature, 201 (1964) 68.
15 F. L. Chen, O. T. Sørensen, G. Y. Meng and D. K. Peng, J. Thermal Anal., 49 (1997) 1255.
16 K. K. Kelley, Bur. Mines Bull., No. 371 (1934).
17 K. K. Kelley and C. T. Anderson, Bur. Mines Bull., No. 384 (1935).
18 A. Finkelstein, Ber., 39 (1906) 1585.
19 L. Hackspill and G. Wolf, Compt. Rend., 204 (1937) 1820.
20 E. H. Baker, J. Chem. Soc. (1964) 699.
21 E. S. Freeman and B. Carroll, J. Phys. Chem., 62 (1958) 394.
22 U. Patnaik and J. Muralidhar, Thermochim. Acta, 274 (1996) 261.
23 M. D. Judd and M. I. Pope, J. Thermal Anal., 4 (1972) 31.